ISBN 978-82-8208-079-8

Investigation of the performance of PVC-Concrete prop for Mine Supports

Shatadru Kundu & Sreenivasa Rao Islavath
Indian Institute of Technology Kharagpur, Kharagpur, India
shatadrukundu@gmail.com *(islavathsreenivas@gmail.com)*

Abstract

The underground mines are protected by various support systems such as wooden and steel props, steel bolts, cable bolts, shield supports and others. During development and depillaring of panels, these supports are installed to carry the load, give the indication for withdrawing men and machinery and to serve for longer duration. The conventional supports especially wooden and steel props, carries lower load and do not give proper indication. In order to meet the underground mines expectation, a new PVC concrete based support prop which carries higher load and possessing ductile behavior is developed in the laboratory. For this, few PVC concrete props of 0.575m, 0.578m and 2m length and having 3”, 5” and 6” diameter were prepared and tested under Uniaxial Compression Test. In this study, the concrete of M10, M15 and M20 grades were prepared to develop the support props. From the laboratory results, it is found that the compressive strength of 25.82 MPa and 25.5 MPa are observed, and maximum displacement of 13.18 mm and 14.11 mm is observed after attaining the peak load. So, all these samples exhibit the ductile behavior. Also, an extensive numerical modelling of developed support props surrounded with underground mine excavation was conducted to estimate the behavior of the PVC-concrete props. All these numerical analyses carried out in elasto-plastic medium. This analysis showed the promising results to use the developed support props as support system in the underground mine.

Keywords

PVC concrete prop, support system, stress, deformation, underground mine

ISRM

NBG

1 Introduction

Underground mines require various supports like rockbolts, girders, shotcrete, props etc. to improve the safety to deploy men and machinery for excavation of mineral deposits. The supports play a key role in making the underground structure stable by controlling deformation caused by induced underground excavation. Key factors affecting mine structures are rock strength, roof span and the forces that are transmitted to the mine roof (Meng et al., 2014; Chang et al., 2013; Tan et al., 2017). The instability of roof can occur due to various factors like unfavourable geological features, development of high stress, incorrect sequence of mining, poor physical properties of rocks and excess ground water pressure (Chen, 1994; Putra, 2021).

The type of supports required to strengthen the underground excavation further depends on the characteristics and strength of the rock masses present in that geological area and also size of excavation. In the continuous miner technology or bord pillar method, the coal is extracted from the slices, leaving the ribs between two slices to support the workings as a natural support. About 25% to 30% of coal is left in the ribs in typical bord and pillar workings. If the support system serves for a longer duration, controls the deformation, and takes the load, then the coal from the rib pillars can also be exploited (Islavath and Bodakunta, 2022).

The prop is one of the most important supports to ensure stability and proper functioning of underground support system. When the hydraulic support is impacted by roof load, it gets prone to deformation, expansion of structural cracks and may fail. Traditionally wooden based support systems such as wooden props and cogs and steel-based support systems like rockbolts, steel arches, and steel cogs have been used. The wood-based support system carries less load (3 to 5 tons) (Li et al., 2011; Tan et al., 2017) due to its weak in nature, and most of the time, these supports may subject to decay process and yield in shorter duration due to water seepage and other mine conditions (Jiao et al., 2013; Wang et al.,2000, 2013, 2014). These supports will be obtained by the process of cutting a few thousands of trees and enhance deforestation (Yan et al., 2014; Gligoric et al., 2022). The steel-based supports are made of Iron ore, which is a non-renewable energy resource and is depleted every year. This support system requires immense energy for manufacturing in particular shape and size. This adds to the cost per tonne of coal produced from underground. The steel bolts and arches will not be recovered after installation and will be left in the workings after the coal extraction (Yu et al., 2019). On a few occasions, the steel props will be recovered and deployed in another working face.

However, as mining techniques have become more sophisticated and scale of operations expanded, the limitations and vulnerabilities of wooden supports became apparent. The need for more robust and reliable support systems led to the exploration of alternative materials and designs. Concrete, Polyvinyl chloride (PVC) pipes, glass fibres etc. have emerged as notable materials in the construction of prop supports, each offering distinct advantages that addresses the shortcomings of traditional wood supports (Havez et al., 2016). PVC has high corrosion resistance, durability and a good strength-weight ratio making it a potential support to be used along with the strong concrete (Saad et al., 2012). Concrete, with its high compressive strength and durability, provides long-lasting strength and support stability capable of withstanding substantial loads and harsh underground conditions. Its resistance to fire and decay makes it an ideal choice for enhancing the safety and longevity of mining infrastructure. PVC, on the other hand, offers a lightweight and corrosion-resistant alternative that is easy to handle and install. Its flexibility and resilience make it suitable for various mining environments, providing reliable support while reducing the overall weight and transportation costs. Hence, a combination of concrete and PVC props are developed and investigated its performance through few laboratory tests for concrete samples to check its behaviour used in the PVC concrete props. Also, 2D numerical models consisting of mine gallery and PVC concrete prop are developed to understand the behaviour of the developed support system.

2 PVC Concrete Prop Preparation

For PVC concrete prop preparation, PVC pipes were procured and concrete was prepared on-site. PVC pipes of 5-inch and 6-inch diameter were used for preparation of prop. Each pipe has two wall thickness of 5 mm and 6 mm.

The estimate of concrete quantity was calculated in terms of weight based on the grade of concrete and size of PVC prop. PVC pipe specifications and concrete quantity estimate are given in Tables 1 and 2 respectively.

Table 1. Specifications of PVC Pipe & Concrete Quantity Estimate

Parameter	6" Pipe measurement	5" Pipe measurement
Inner diameter of PVC pipe	0.1524 m (6")	0.1270 m (5")
Area of the PVC pipe	0.01825 m^2	0.01267 m^2
Length of PVC Pipe	2 m	2 m
Volume of Wet Concrete in Pipe	0.03650 m^3	0.02535 m^3
Concrete Density (PCC)	2400 kg/m^3	2400 kg/m^3
Weight of concrete required (minimum)	87.594 kg	60.289 kg
Concrete weight estimated taking losses into account	120 kg	90 kg
PVC Density	1400 kg/m^3	1400 kg/m^3
Youngs modulus of Elasticity of PVC	4 GPa	4 GPa
Poissons ratio of PVC	0.4	0.4

Table 2. Estimation of Material quantity for preparing Concrete

Concrete Grade	Nominal Mix Ratio	Cement Weight (kg)	Sand Weight (kg)	Aggregate Weight (kg)	Water (l)	Water-Cement Ratio
M10	1:3:6	6.08	18.25	36.50	3.04	0.5
M15	1:2:4	8.69	17.38	34.76	4.34	0.5
M20	1:1.5:3	15.93	23.89	47.78	7.64	0.48
M25	1:1:2	21.90	21.90	43.80	10.07	0.46

The concrete was prepared by mixing cement, sand and aggregates in proportion as per nominal mix specification given by IS 456 with the aid of water. The prepared concrete, before hardening, was poured into the PVC pipe without delay, vertically from one of the openings of the pipe. Fig.1 shows the preparation of PVC-concrete props samples for testing.

Fig.1. Concrete preparation & filling it in hollow PVC pipes to prepare the PVC concrete prop support

The prepared PVC concrete pipes along with cubical concrete blocks were then subjected to curing for 28 days by immersing under water in an artificially prepared pond that was prepared by aligning bricks of desired dimensions and then place a polythene sheet as surface. The concrete blocks which would be used in lab for testing parameters of concrete were also kept under curing along with it. Fig.2 shows the curing process of PVC concrete props and concrete blocks.

Fig.2.Curing of PVC concrete prop and concrete blocks

3 Smaller Concrete Sample Preparation

Concrete cube samples for concrete property investigation were prepared in cubical moulds of dimensions 150 mm x 150 mm x 150 mm by pouring concrete in it and vibrated by a vibrating table and left to harden for 24 hours. Then, it is subjected to curing in the artificially prepared pond at work site for 28 days as per code provisions. After curing, they were subjected to coring, cutting and polishing so that cylindrical shape could be attained and easier to compare with concrete in PVC props. A core drill of 54 mm diameter was used to recover a cylindrical sample. The length of the core varied between 2.5-3 times the diameter of the concrete core. The core was prepared for every grade of concrete - M10, M15, M20 and M25. Six cores were extracted from each grade of concrete cubes in total. Thus, a total of 24 samples of concrete cores were prepared. Fig.3 shows the preparation of samples to estimate the physico-mechanical properties of concrete.

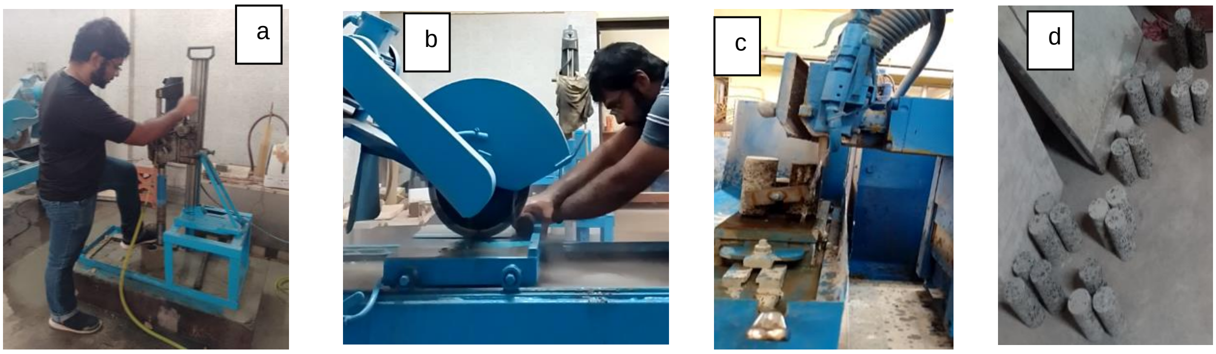

Fig.3.a Coring b. Cutting Concrete samples. c. Polishing samples. d. Prepared concrete samples

4 Laboratory Testing

The smaller cylindrical concrete samples were tested in laboratory to determine the properties of concrete such as cohesion, angle of internal friction, modulus of elasticity, poissons ratio, compressive strength and density. These properties of concrete were further used for numerical modelling to analyse real time behaviour of PVC concrete props. Samples were soldered with strain gauge and tested in UTM. A total of 8 samples were subjected for UCS Test and 12 samples for Triaxial Test. Fig.4a and 4.b. shows the samples being tested under UTM for UCS test and failed sample after test respectively

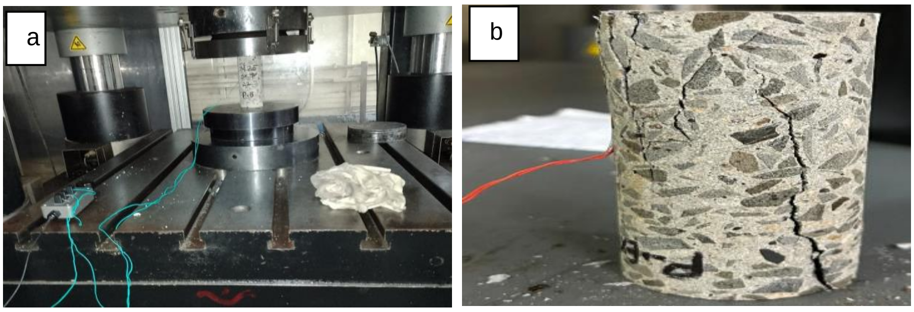

Fig.4. a. Sample under testing. b. Failed sample under UCS test

To estimate cohesion and angle of internal friction of concrete samples, Triaxial tests were performed at confining pressures of 1 MPa, 2 MPa and 4 MPa. Fig.5 depicts the samples tested under triaxial test.

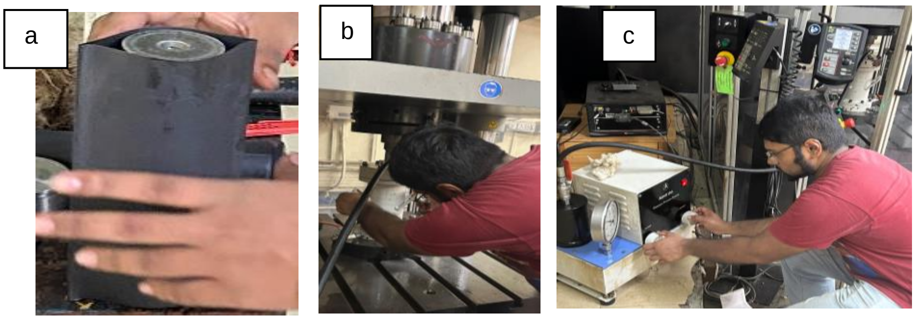

Fig.5. a. Encasing sample with latex. b. Fixing sample with oil filled steel mould and confining it tightly. c. Fixing arrangement with INSTRON UTM.

5 RESULTS of Laboratory Tests

5.1 UCS Test

From the UCS tests as given in Table 3, it is found that the maximum compressive strength of 30.53 MPa is attained for M25 sample and a minimum of 13.26 MPa is attained for M10 sample. The modulus of elasticity varied from 2.75 GPa to 8.88 GPa. Also, poisons ratio is observed minimum of 0.103 for M25 concrete samples and maximum of 0.217 for M10 concrete samples. Fig.6 shows the stress-strain behaviour of concrete samples under UCS Test.

Table 3. Results of UCS Test showing obtained Compressive Strength, Elastic Modulus and Poissons Ratio of concrete

Concrete Grade	Diameter (mm)	Height (mm)	Maximum Compressive Load (kN)	Compressive Strength (MPa)	Elastic Modulus (GPa)	Poisson's Ratio
M25	53.68	129.69	69.10	30.53	8.88	0.103
M20	53.60	131.33	54.17	24.01	5.55	0.118
M15	53.67	135.31	40.42	19.19	3.84	0.145
M10	53.73	133.21	30.06	13.26	2.75	0.217

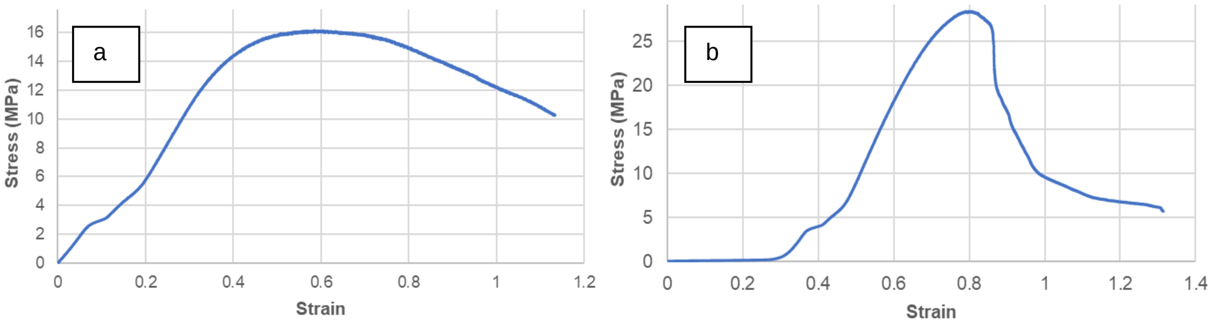

Fig.6.Stress-Strain graphs for UCS test samples a. M10 b. M25

5.2 Triaxial Test

As mentioned in the above section, triaxial tests are performed at 1 MPa, 2 MPa and 4 MPa confining stress. The results of Triaxial tests are given in Table 4. The obtained major principal stresses were maximum for M25 with 59.26 MPa and minimum for M10 with 25.13 MPa. The elastic modulus for the samples varied between 2.34 MPa to 7.81 MPa. The average cohesion and angle of internal friction values of concrete samples are observed as 4.72 MPa and 40.93^0 respectively. Fig.7 shows the variation of Major and Minor Principal stresses observed during testing. During testing, it was observed that concrete strength increased and time to attain its peak strength improved with better grade of concrete.

Table 4. Results of Triaxial Test with Estimated Cohesion & Angle of Internal Friction values

Concrete Grade	Minor Principal Stress (MPa)	Major Principal Stress (MPa)	Cohesion (MPa)	Angle of Internal Friction (degrees)
M10	1	25.13	3.71	36.46
M15	2	36.08	4.58	38.45
M20	4	45.35	5.66	44.13
M25	4	59.26	6.38	47.86

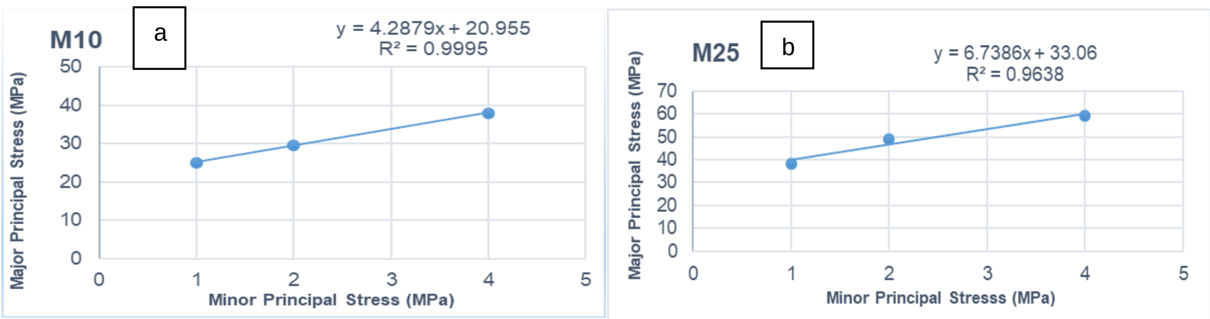

Fig.7. Graphs plotted to estimate cohesion and angle of internal friction of concrete

5.3 Behaviour of PVC Concrete Prop

Few tests for UCS were conducted with 3" pipes having M10 grade for determining properties of PVC-concrete props. Fig.8 shows the stress-strain behaviour of the 3" PVC-concrete props where a stress of 25.82 MPa after developing a displacement of 13.18 mm.

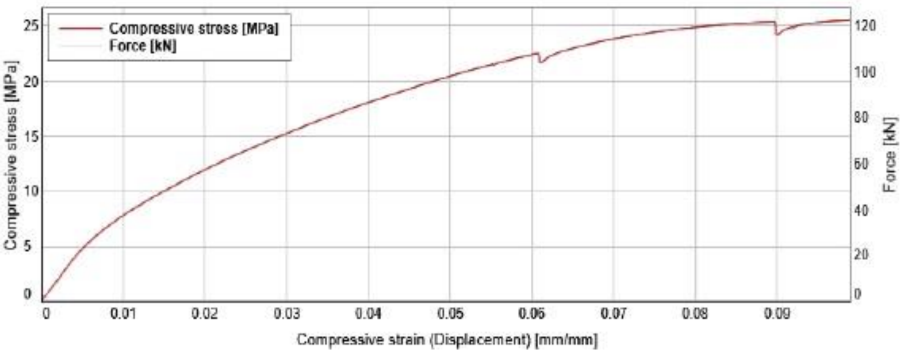

Fig.8. Stress-Strain graph for the tested sample of PVC concrete prop

This means that after attaining the peak load, the prop continues to hold the roof displacement for a reasonable amount of time. The PVC confines the concrete and prevents it from an instantaneous brittle failure. On vertical loading, concrete tends to deform outwards but PVC resists from deforming by confining it inwards. As a result, a huge amount of shear stress is exerted on the peripheral PVC. Hence, displacement and stress both come out to be slightly greater on the PVC pipe compared to the inner concrete which itself is protected by the PVC pipe.

6 Numerical Modelling

6.1 Model Development

2D finite element models are developed to understand the effectiveness of PVC concrete prop installed in the mines. For this, a pillar of 40 m size surrounded by galleries of 5 m x 3 m is developed. A coal seam of 5m thickness is situated at 300 m beneath the surface. An overburden layer of 300 m thick sandstone over coal seam and 100 m thick sandstone below coal seam were developed. The size of the model is 1050 m x 405 m. Two props in each gallery at 0.5 m from the sides are installed. A total of 3 variations are modelled in this study. In each variation, cohesion of concrete is modified as 5 MPa, 6.25 MPa and 7.5 MPa. All the models are analysed in elasto-plastic condition using Mohr-Coulomb failure criterion. Fig.9 shows the model developed for stability analysis.

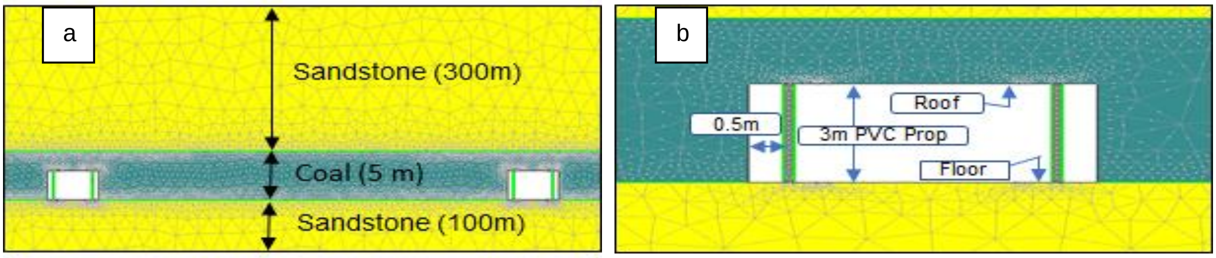

Fig.9. Model prepared & meshed with coal layer between sandstone layers (left) and sectional view of props in model (right)

6.2 Results and Discussion

6.2.1 Vertical Stress Distribution

Fig.10 depicts the vertical stress distribution along path considered in the roof under No Prop and Prop conditions pointing the difference in prop behaviour in the two conditions. The corners of pillar are found to develop greater vertical stress which reduces towards the core of the pillar. The vertical stress ranges from 6.85 MPa to 7.88 MPa on the pillars.

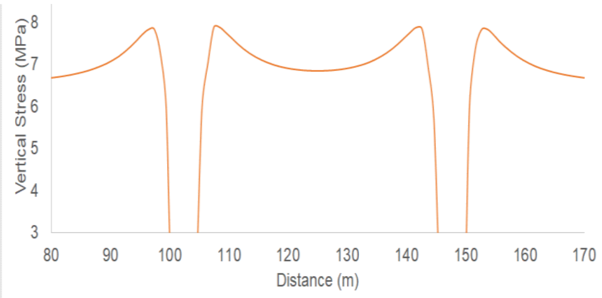

Fig.10. Vertical stress distribution around the pillars

6.2.2 Major and Minor Principal Stress Distribution

Figures 11a and 11b show the development of major and minor principal stress distribution. It can be observed that major principal stress of 10.26 MPa and minor principal stress of 6.69 MPa are developed in roof in No Prop condition. However, the minor principal stress around the roof improves to 6.72 MPa after the installation of props as shown in Fig.12. This may enhance the binding of roof rock layers.

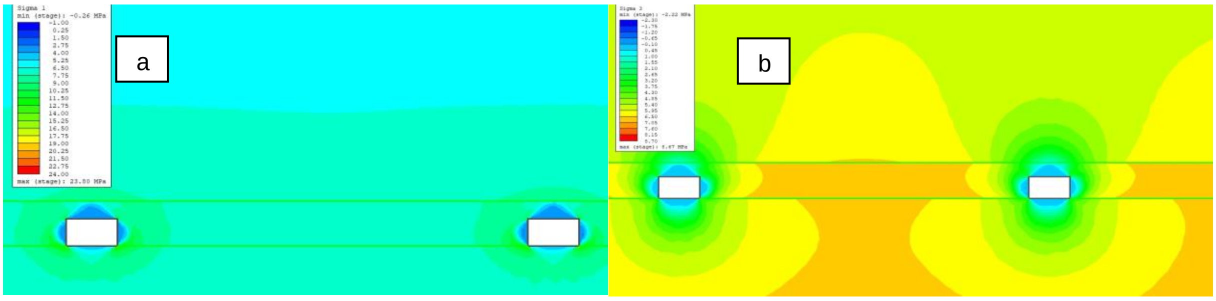

Fig.11. NO PROP condition. a. Major Principal Stress. b. Minor Principal Stress

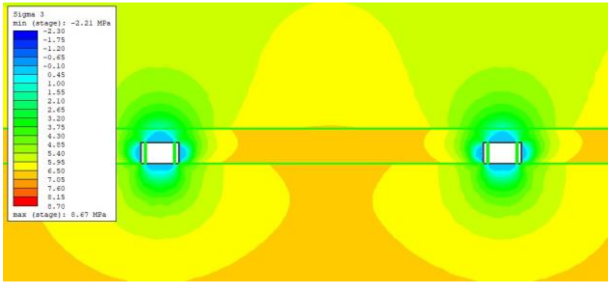

Fig.12.Minor Principal Stress around the roof of pillar in PROP condition

6.2.3 Roof Convergence

The roof convergence at prop locations is estimated for three different conditions. Fig.13. describes the roof convergence occurrence in those conditions. From the figure, it can be clear that roof convergence of 2 mm to 3 mm is reduced if a prop of 6-inch diameter is installed in the mine.

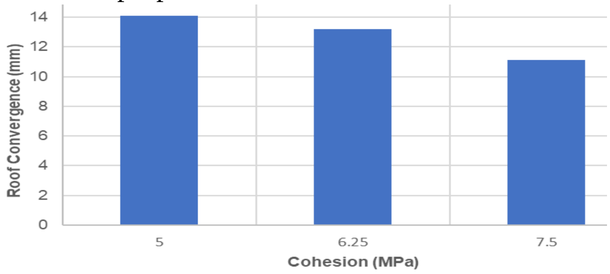

Fig.13. Displacement variation with cohesion of concrete

6.2.4 Safety Factor

The safety factor of roof is estimated based on Mohr's-Coulomb failure criterion. After the analysis of results, it is found that safety factor of 3.08, 3.66 and 4.23 is observed at the installed location of developed support system for 5 MPa, 6.25 MPa and 7.5 MPa models respectively. However, in No Prop condition, the safety factor of roof at that installed location is observed less than 1. Also, it is observed that the safety factor of pillar varies from 4.11 to 5.37. It shows that the developed support system installed in the mine can give promising results since it improves safety factor. Fig.14 shows the increasing variation of safety factor with cohesion of concrete.

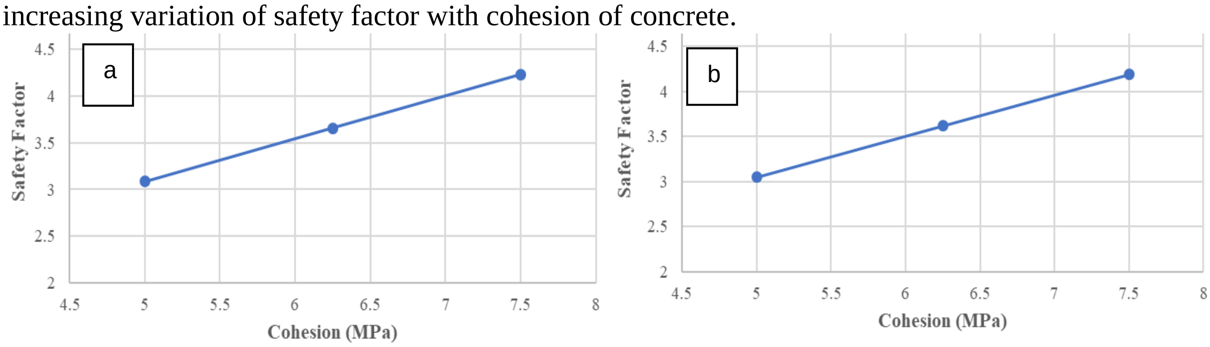

Fig.14.Safety Factor variation with cohesion of concrete for a. Query 1. b. Query 2

7 Conclusions

The results presented in this paper highlights the development and evaluation of PVC-concrete-based support props as a novel solution for underground mine support systems. Laboratory testing of the developed props demonstrated promising mechanical properties, including higher load-carrying capacity and notable ductile behaviour, with compressive strengths ranging from 15.54 MPa to 20.48 MPa and maximum displacements from 11.10 mm to 14.11 mm after attaining peak load. These results confirm the potential of PVC-concrete props to address the limitations of traditional wooden and steel supports, particularly in terms of load-bearing efficiency and deformation.

The numerical modelling of the PVC-concrete props within an elasto-plastic medium further investigated their capability to perform effectively under the actual mining environment. The numerical results show that improving the safety factor from 0.65 to 4.13 and reducing deformation by about 2 mm to 3 mm. Thus, PVC-concrete props can have capabilities to be used as support system by replacing the conventional support system.

References

Gligoric M, Gligoric Z, Lutovac S, Negovanovic, M, Langovic Z (2022). Novel Hybrid MPSI–MARA Decision-Making Model for Support System Selection in an Underground Mine. Systems 2022, 10(6), 248; https://doi.org/10.3390/systems10060248

Chen D (1994). Design of Rockbolting System of Underground Excavation. University of Wollongong (Thesis Collection). Australia.

Putra RAM (2021). Underground Support System Determination: A Literature Review.

Islavath SR, Bodakunta S (2022). Estimation of Optimum Line of Extraction for Continuous Miner Workings and Development of Continuous Miner Stability Index (CMSI) using 3D Numerical Modelling and Statistical Approach. Mining, Metallurgy & Exploration, Volume 39, pages 1149–1169.

Havez AA, Wahab N, Al-Mayah A, Soudki KA (2016). Behaviour of PVC encased reinforced concrete walls under eccentric axial loading. Structures, Volume 5, Pages 67-75

Yu T, Zhao H, Ren T and Remennikov A (2019). Novel hybrid FRP tubular columns with large deformation capacity: Concept and behavior. Composite Structures, 212, 500-512.

Jiao YY, Song L, Wang X, Coffi A (2013). Improvement of the U-shaped steel sets for supporting the roadways in loose thick coal seam. International Journal of Rock Mechanics and Mining Sciences, 60, 19–25. https://doi.org/10.1016/j.ijrmms.2012.12.038

Saad NA, Al-Maamory MH, Mohammed MR, Hashim AA (2012). The Effect of Several Service and Weathering Parameters on Tensile Properties of PVC Pipe Materials. Materials Sciences and Applications, 2012, 3, 784-792. http://dx.doi.org/10.4236/msa.2012.311114

Li X, Yao Q, Man J, Chen C, He L (2011). Development of fractures in soft rock surrounding a roadway and their control. Mining Science and Technology (China), 21, 573–579.

Tan X, Chen W, Liu H, Chan AHC, Tian H, Meng, X, Wang F, and Deng X (2017). A combined supporting system based on foamed concrete and U-shaped steel for underground coal mine roadways undergoing large deformations. Tunnelling and Underground Space Technology, Vol 168, 196-210.

Yan L and Chouw N (2014). Natural FRP tube confined fibre reinforced concrete under pure axial compression: A comparison with glass/carbon FRP. Thin-Walled Structures, 82, 159–169.

Wang C (2000). The optimal support intensity for coal mine roadway tunnels in soft rocks. International Journal of Rock Mechanics and Mining Sciences, 37, 1155–1160. https://doi.org/10.1016/S13651609(00)00044-7

Wang FT, Tu SH, Yuan Y, Feng YF, Chen F, Tu HS (2013). Deep-hole pre-split blasting mechanism and its application for controlled roof caving in shallow depth seams. International Journal of Rock Mechanics and Mining Sciences, 64, 112–121. https://doi.org/10.1016/j.ijrmms.2013.08.026

Wang, ZL, Chen, XX, Xing SR (2014). Study on stress field distribution characteristics under coal seam pre-splitting blasting. Procedia Engineering. 84, 913–919. 10.1016/j.proeng.2014.10.515.